ORNL/CP-101210

# MODELING OF MICROSTRUCTURE EVOLUTION IN AUSTENITIC STAINLESS STEELS IRRADIATED UNDER LIGHT WATER REACTOR CONDITIONS

J. Gan*, G.S. Was**, R.E. Stoller***
*NERS Department, University of Michigan, Ann Arbor, MI 48109, ganjian@engin.umich.edu
**NERS Department and MSE Department, University of Michigan, Ann Arbor, MI 48109
***Metals and Ceramic Division, Oak Ridge National Laboratory, Oak Ridge, TN 37831



## ABSTRACT

A model for the development of microstructure during irradiation in fast reactors has been adapted for light water reactor (LWR) irradiation conditions (275 ~ 325 °C, up to ~10 dpa). The original model was based on the rate-theory, and included descriptions of the evolution of both dislocation loops and cavities. The model was modified by introducing in-cascade interstitial clustering, a term to account for the dose dependence of this clustering, and mobility of interstitial clusters. The purpose of this work was to understand microstructural development under LWR irradiation with a focus on loop nucleation and saturation of loop density. It was demonstrated that in-cascade interstitial clustering dominates loop nucleation in neutron irradiation in LWRs. Furthermore it was shown that the dose dependence of in-cascade interstitial clustering is needed to account for saturation behavior as commonly observed. Both quasi-steady-state (QSS) and non-steady-state (NSS) solutions to the rate equations were obtained. The difference between QSS and NSS treatments in the calculation of defect concentration is reduced at LWR temperature when in-cascade interstitial clustering dominates loop nucleation. The mobility of interstitial clusters was also investigated and its impact on loop density is to reduce the nucleation term. The ultimate goal of this study is to combine the evolution of microstructure and microchemistry together to account for the radiation damage in austenitic stainless steels.

## INTRODUCTION

Radiation induced microstructure changes in austenitic stainless steels in LWR cores is suspected as a cause for irradiation assisted stress corrosion cracking (IASCC). Without fully understanding the microstructure evolution under irradiation, it will be impossible to understand the role of microstructure in IASCC in LWRs. The purpose of this work is to adapt an existing microstructure model which was developed for fast reactors and to apply it to the evolution of the dislocation loop structure under irradiation conditions relevant to LWRs. The details of the fast reactor microstructure model which was chosen for this study can be found in references[1, 2]. Both QSS and NSS treatments of the calculation of point defect and interstitial cluster concentrations are discussed in this work. The effect of mobility of small interstitial cluster on the microstructure evolution is also addressed. The original model simulated the evolution of the dislocation structure, cavities and transient vacancy clusters formed by cascade collapse. The dislocation component of the model included both thermal and radiation-induced mechanisms for dislocation formation and recovery. The formation and growth of Frank faulted interstitial loops provided the primary source term for the dislocation network. The time dependence of the extended defects, including in-cascade vacancy clusters was explicitly included in the rate equations describing their evolution. In the original model, the small interstitial clusters were able to form only by classical nucleation. One important feature of the model was a detailed accounting of the fate of all the point defects.

"The submitted manuscript has been authored by a contractor of the U. S. Government under contract No. DE-AC05-96OR22464. Accordingly, the U.S. Government retains a nonexclusive, royalty-free license to publish or reproduce the published form of this contribution, or allow others to do so, for U.S. Government purposes."

## DISCLAIMER

## DESCRIPTION OF THE MODEL

The focus of this work was on microstructure evolution of the faulted dislocation loops which are the dominant defects in austenitic stainless steels irradiated under LWR conditions [3]. The evolution of the cavity structure was included, but cavity nucleation was not addressed in the model. The model assumed that the tetra-interstitial is the stable nucleus for a Frank loop. The sink terms for the point defects and mobile defect clusters consist of the subgrain structure, bubbles and voids, transient vacancy clusters in the form of micro-voids as a result of cascade collapse, network dislocations, and Frank dislocation loops. The maximum loop size is controlled by geometric constraint and unfaulting occurs when a loop encounters another loop or network dislocation. The rate equations used for point defect and cluster concentrations are:

$$\frac{dC_v}{dt} = G_v - \beta_v^2 C_2 - \beta_v^3 C_3 - \beta_v^4 C_4 - \alpha C_i C_v - D_v C_v S_v^T \quad (1)$$

$$\frac{dC_i}{dt} = G_i + C_2(2E_2^i + \beta_v^2 - \beta_i^2) + C_3(E_3^i - \beta_i^3) - \beta_i^1 C_i - \beta_i^4 C_4 - \alpha C_i C_v - D_i C_i S_i^T \quad (2)$$

$$\frac{dC_2}{dt} = \eta \mathbf{G_{dpa}} \frac{\mathbf{f_{i2}}}{\mathbf{2}} \mathbf{exp(-k*\phi)} + \beta_i^1 \frac{C_i}{2} + C_3(\beta_v^3 + E_3^i) - C_2(\beta_v^2 + \beta_i^2 + E_2^i) - \mathbf{D_{i2} C_2 S_i^T} \quad (3)$$

$$\frac{dC_3}{dt} = \eta \mathbf{G_{dpa}} \frac{\mathbf{f_{i3}}}{\mathbf{3}} \mathbf{exp(-k*\phi)} + \beta_i^2 C_2 + \beta_v^4 C_4 - C_3(\beta_v^3 + \beta_i^3 + E_3^i) - \mathbf{D_{i3} C_3 S_i^T} \quad (4)$$

$$\frac{dC_4}{dt} = \eta \mathbf{G_{dpa}} \frac{\mathbf{f_{i4}}}{\mathbf{4}} \mathbf{exp(-k*\phi)} + \beta_i^3 C_3 - \beta_v^4 C_4 - C_4 \tau_4^{-1} - \mathbf{D_{i4} C_4 S_i^T} \quad (5)$$

$$G_v = \eta G_{dpa}(1-\chi) + D_v \sum S_v^j C_v^j \quad (6)$$

$$G_i = \eta G_{dpa}(1 - (\mathbf{f_{i2}} + \mathbf{f_{i3}} + \mathbf{f_{i4}})\mathbf{exp(-k*\phi)}) \quad (7)$$

The original fast reactor model is modified for LWR conditions by adding the terms shown in bold type. The $C_2$, $C_3$ and $C_4$ are the concentrations of di-, tri- and tetra-interstitial clusters, respectively. The $\beta_v^j$ and $\beta_i^j$ (j=2, 3, 4) are the rate constant for impingement of vacancies and interstitials on the interstitial cluster of size j. $E_2^i$ and $E_3^i$ are the rate constant for emission of a single interstitial from di- and tri-interstitial clusters. $G_v$ and $G_i$ are the point defect generation rates. $S_v^T$ and $S_i^T$ are the total sink strengths for point defects. $D_{i2}$, $D_{i3}$ and $D_{i4}$ are the diffusivities for di-, tri- and tetra-interstitial clusters. In Eqn. 6, $\eta$ is the cascade efficiency and $\chi$ is the fraction of cascade vacancies collapsed into micro-voids. In Eqn. 2-7, $f_{i2}$, $f_{i3}$ and $f_{i4}$ are the fraction of cascade interstitials staying in the form of interstitial clusters. In Eqn. 7, $\phi$ is dose in dpa and k is a constant introduced here for the dose dependence of the defect clustering which follows a similar treatment as in Makin's theory for the saturation of depleted zones [4]. The other terms have their usual meanings and a more complete description of the original model and the input parameters can be found in ref. [2]. The major parameters used to distinguish the difference between fast reactor and LWR are listed in table 1.

Table 1. The different irradiation conditions

| | Fast reactor | LWR |
|---|---|---|
| temperature ( °C ) | 350 ~ 750 | 275 ~ 325 |
| dose rate (dpa/s) | $10^{-6}$ | $10^{-8}$ |
| helium rate (appm/dpa) | 0.35 | 3.5 |

In this work, a QSS treatment is used first to simulate the LWR case. The effect of in-cascade interstitial clustering as well as its dose dependence is evaluated by comparison between model calculation and measurement of loop density and diameter. Then the NSS treatment is used and the result is compared with QSS treatment. The effect of mobility of the small interstitial clusters on the loop density is addressed last.

## QUASI-STEADY STATE TREATMENT

In this case the concentration of point defects and interstitial cluster $C_2$, $C_3$ and $C_4$ were calculated assuming quasi-steady-state. The defect concentrations $C_v$, $C_i$, $C_2$, $C_3$ and $C_4$ were calculated by setting the time derivative terms in Eqn.. 1-5 equal to zero. The calculation was repeated at each time step assuming a QSS each time. The loop density and diameter as a function of dose were calculated at T=275 °C without in-cascade interstitial clustering ($f_{i2}$, $f_{i3}$, $f_{i4}$=0) and the comparison with the LWR data trend is shown in Fig 1a. Due to the lack of a comprehensive data set for LWR core conditions, a data "trend" was established by using published values of loop density and diameter at higher temperature (375-400 °C) and scaling the density higher and the size lower to account for the lower temperature [3]. The large discrepancy between the calculation and the data indicates a severe underestimation of the loop nucleation if loop nucleation occurs only by diffusive clustering of point defects. This difference cannot be resolved by adjusting irradiation and material parameters within their reasonable ranges, and indicates that another nucleation mechanism takes place. By adding the in-cascade interstitial clustering as shown in the first term in Eqn.. 3-5 as well as the term shown in Eqn. 7, the calculation with in-cascade interstitial clustering ($f_{i2}$, $f_{i3}$, $f_{i4}=10^{-5}$, k=0) is also shown in Fig 1a to provide reasonable agreement between model and data. Even the low values chosen for $f_{i2}$, $f_{i3}$ and $f_{i4}$ have a strong effect on the loop density because clustering provides a direct nucleation path within the cascade. Fig 1b shows the loop diameter as a function of dose for calculations with and without in-cascade interstitial clustering along with the data trend. The model predication and data trend appear to show similar behavior in size saturation.

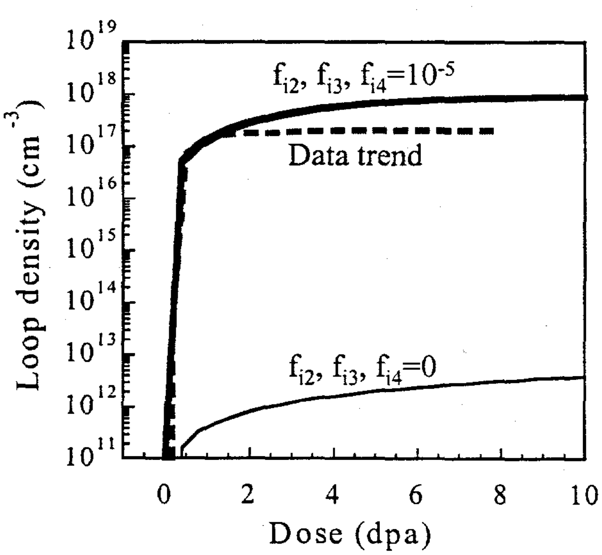


Fig 1a. Calculated loop density with and without in-cascade interstitial clustering in comparison with data trend.

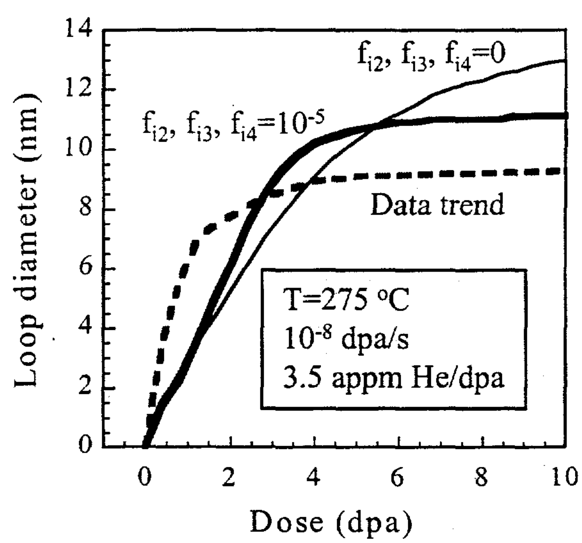


Fig 1b. Calculated loop diameter with and without in-cascade interstitial clustering in comparison with data trend.

A closer look at loop density as a function of dose for the in-cascade interstitial case shows that the loop density increases continually up to 10 dpa without showing quick saturation behavior. This is not what was shown by the measurements. Following Makin's theory for the saturation of depleted zones, a dose dependence term ($e^{-k*\phi}$, k≠0) was added to the production of in-cascade interstitial clusters as shown in Eqns. 3-5 and Eqn.7. Assuming in-cascade interstitial clustering drop to 50% of its initial value at 1 dpa, then the corresponding constant is k=0.7. Including this dose dependent term in the calculation results in an improved agreement between model and data for loop density, fig. 2a. The corresponding change in loop diameters due to dose dependence of in-cascade interstitial clustering is shown in fig. 2b.

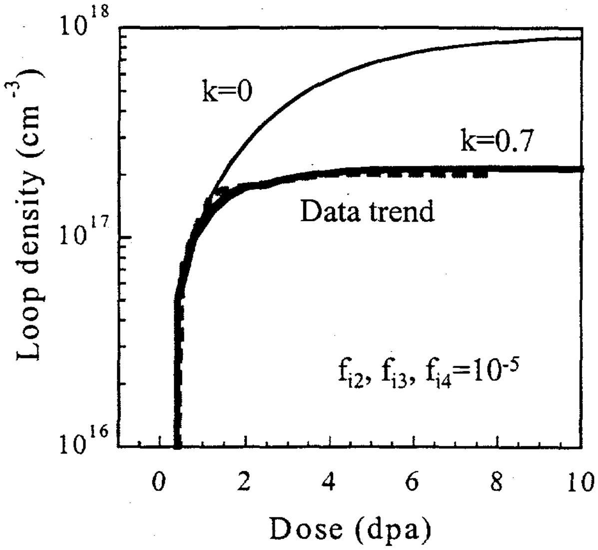


Fig 2a. Calculated loop density with and without dose dependence of in-cascade clustering in comparison with data trend.

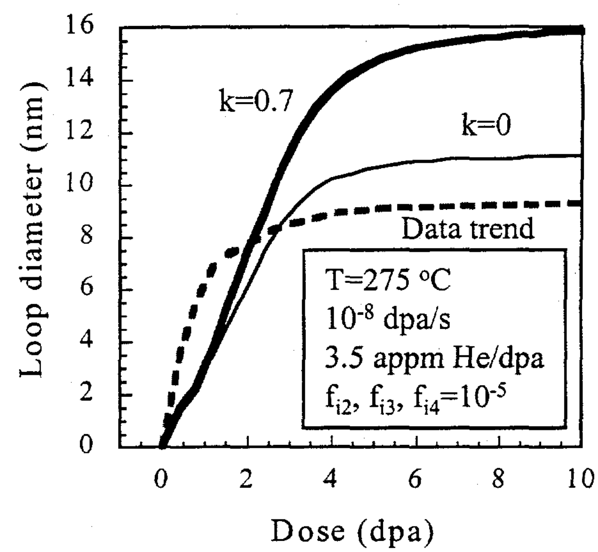


Fig 2b. Calculated loop diameter with and without dose dependence of in-cascade clustering in comparison with data trend.

**NON-STEADY STATE TREATMENT**

In this treatment, the calculation of defect concentrations is done by explicit integration of the rate equations 1-5. At LWR irradiation temperature, there was a concern that the QSS treatment for the calculation of defect concentration may not be adequate. The use of the QSS solution at lower temperatures was previously shown to reduce the calculated loop density [5]. However model calculations show that at lower temperature the difference between QSS and NSS treatments is reduced when the in-cascade interstitial clustering is added. Fig 3a shows that at T=275 °C, the difference between QSS and NSS treatments on the faulted loop density is large when the in-cascade interstitial clustering is not included, but the two give nearly the same results when in-cascade interstitial clustering is introduced. When loop nucleation is dominated by in-cascade interstitial clustering, the higher point defect concentration calculated using the NSS method shows virtually no effect on loop density. The decrease of loop density with dose in the NSS ($f_{i2}$, $f_{i2}$, $f_{i2}=0$) case is due to the fast build-up of faulted loops that increases the total sink strength, therefore suppressing the loop nucleation. Similarly for loop size as shown in Fig 3b, at doses above 5 dpa, both treatments give the same results for $f_{i2}$, $f_{i2}$, $f_{i2}=10^{-5}$.

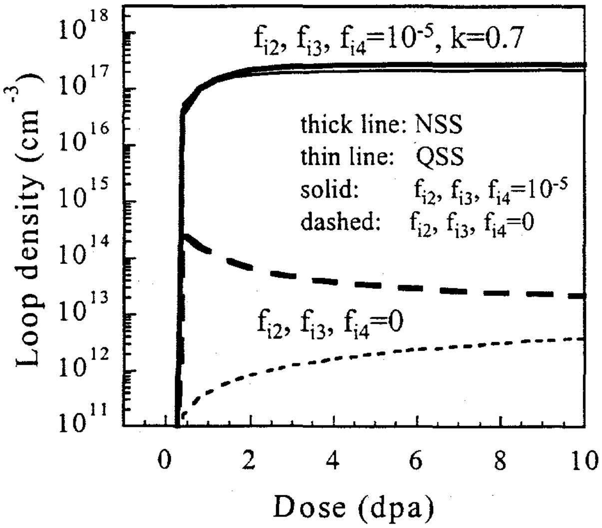


Fig 3a. Comparison of quasi-steady-state (QSS) and non-steady-state (NSS) treatment in calculation of loop density with and without in-cascade interstitial clustering.

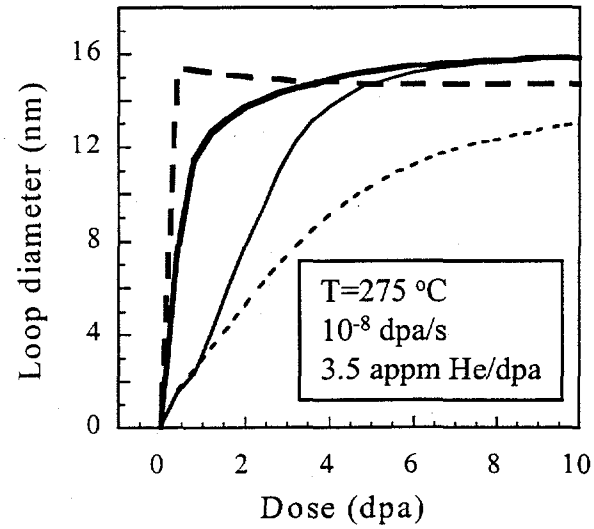


Fig 3b. Comparison of quasi-steady-state (QSS) and non-steady-state (NSS) treatment in calculation of loop diameter with and without in-cascade interstitial clustering.

## INTERSTITIAL CLUSTER MOBILITY

The effect of interstitial cluster mobility on loop density and size was evaluated by adding the last terms as shown in Eqns. 3-5. The mobility of small interstitial clusters introduces additional loss terms to the interstitial clusters $C_2$, $C_3$ and $C_4$. The impact of these loss terms is a reduction in loop density because interstitial clusters can now be lost to sinks [6]. Atomistic simulations have indicated that even relatively large interstitial clusters may migrate with an

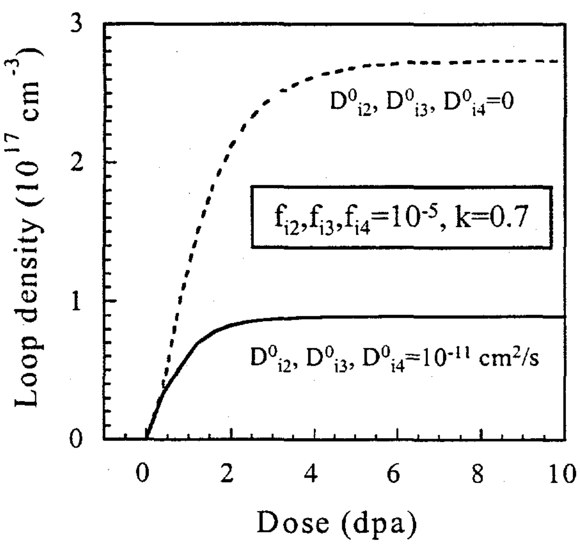


Fig 4a. The effect of interstitial cluster mobility on loop density for LWR case, the calculation was done using NSS treatment.

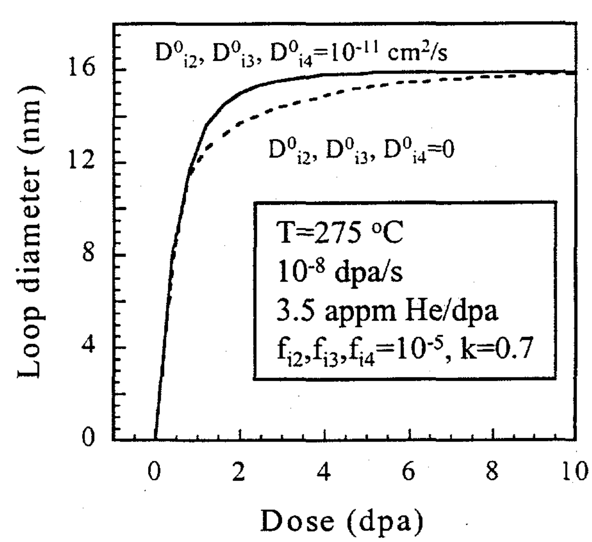


Fig 4b. The effect of interstitial cluster mobility on loop diameter for LWR case, the calculation was done using NSS treatment.

activation energy as low as that for single interstitial [7]. In addition, these clusters can exhibit one-dimensional, as well as three-dimensional diffusion. Because of these uncertainties, a relatively simple approach was adopted for this initial evaluation, only allowing di-, tri- and tetra-interstitial clusters to move to the sinks and assuming the same activation energy and sink strength as for single interstitials. The results are shown in fig 4a. Note that if the activation energy for interstitial clusters is assumed to be the same as for single interstitials (0.85 eV), the pre-exponential term for interstitial cluster diffusivity must be very low to give results which preserve a trend similar to measurement. It appears that cluster mobility also affects the saturation behavior. The impact of cluster mobility on loop diameter is negligible as shown in fig. 4b, mainly due to its little impact on point defect concentration.

## CONCLUSION

The original model for microstructure development in fast reactors severely underestimated the faulted loop density at LWR irradiation condition. The initial results in this work have shown that Stoller's fast reactor microstructure model can be adapted to LWR case with proper modification and adjustment on both model and input parameters. It was identified that in-cascade interstitial clustering must be included to match the measured data. A dose dependence term ( exp(-dose•k) ) for in-cascade interstitial clustering efficiency is required for good agreement with measured dose dependence of faulted loop density. The trend and magnitude of loop diameter as function of dose is in reasonable agreement between model calculation and measured data. The quasi-steady-state and non-steady-state treatment for defects concentration show nearly no difference on loop density even at T=275 °C when the loop nucleation is dominated by in-cascade interstitial clustering. The impact of cluster mobility on loop is a reduction in density. The simple parametric evaluation of in-cascade clustering and cluster mobility presented here indicates that these mechanisms can have a significant impact on the model predications. For example, an unrealistically low pre-exponential term on the cluster diffusivity was required to maintain reasonable agreement with the data. This implies that the microstructural model requires further modification to properly account for these mechanisms; this work is proceeding.

## ACKNOWLEGEMENTS

Research sponsored at the Oak Ridge National Laboratory by the Division of Materials Sciences and the Office of Fusion Energy Sciences, U.S. Department of Energy under contract DE-AC05-96OR22464 with Lockheed Martin Energy Research Corp.

## REFERENCES

1. R.E. Stoller and G.R. Odette, Effects of Radiation on Materials: Eleventh Conference, ASTM STP 782, H.R. Brager and J.S. Perrin, Eds., 1982. pp. 275-294.
2. R.E. Stoller and G.R. Odette, Radiation Induced Changes in Microstructure: 13th Int. Symp. (Part I), ASTM STP 955, F.A. Garner, N.H. Packan, and A.S. Kumar, Eds., 1987, pp. 371
3. S.J. Zinkle, P.J. Maziasz and R.E. Stoller, J. Nucl. Mat., 206 (1993) pp. 266-286
4. D.R. Olander, Fundamental Aspects of Nuclear Reactor Fuel Elements, ( U.S. Department of Commerce, National Technical Information Center, 1976), p. 435
5. R.E. Stoller, J. Nucl. Mater., 244 (1997) 195-204
6. R.E. Stoller, "Effect of Rad. On Met.: 18th Int. Symp., ASTM 1325, R.K. Nanstad, M.L. Hamilton, F.A. Garner, and A.S. Kumar, Eds., AMST, 1997
7. R.E. Stoller, G.R. Odette, and B.D. Wirth, J. Nucl. Mater. 251 (1997) 49-60